1999-3-J

MEPEG (1999) 8:450-454

An Acoustic Emission Study of Cutting Bauxite Refractory Ceramics by Abrasive Water Jets

A.W. Momber, R.S. Mohan, and R. Kovacevic

(Submitted 30 December 1998; in revised form 26 January 1999)

This article discusses the material removal process in bauxite refractory ceramics cut by abrasive water jets. Several parameters of the process were changed during the experiments. The experiments were monitored online by the acoustic emission (AE) technique. It was found that AE signals are able to sense the material removal process as well as the machining performances very reliably. Unsteady material removal mode consisting of matrix removal and intergranular fracture was very well represented in the AE signals by an unsteady time dependent signal type characterized by burst emissions and a frequency domain signal associated with a twin-peak shape. The particular characteristics of the signal depend on the energy involved in the process.

Keywords abrasive water test, acoustic emission analysis, bauxite, frequency analysis, refractory

1. Introduction

The development of high quality refractory materials by the ceramic industry has brought up latent problems associated with the machinability of the bricks being manufactured. To produce bricks of complex shape, advanced pressing methods, such as hot isostatic pressing, have been introduced. However, this has led to high production costs, and the refractory bricks produced are very expensive.

Abrasive water jet (AWJ) machining could be one possible technology for manufacturing high quality refractory bricks of special shapes and formats because it has a proven capability for cutting, drilling, and milling difficult-to-machine materials, such as ceramics, heat sensitive materials, composites, and glass (Ref 1). There have been only a few investigations on the machinability of refractory ceramics by AWJs. Momber et al. (Ref 2) machined several types of refractory ceramics by AWJ and estimated volume removal capacity and specific energy of the process as well as quality features, such as kerf geometry and wall roughness. Through scanning electron microscopy (SEM), they identified a complex mixed-mode material removal mechanism. Most recently, Kovacevic et al. (Ref 3) performed piercing experiments on glass and refractory ceramics. Although they could show that acoustic emission (AE) is capable of sensing the piercing process reliably, no attempt was made to monitor the failure mechanisms involved in the piercing process directly by AE.

Systematic investigations into AE signals generated during AWJ machining were performed by Mohan et al. (Ref 4, 5) followed by Momber et al. (Ref 6). Using advanced signal processing techniques, these authors detected functional relationships between the AE signals acquired during the cutting and the depth of cut and the energy dissipated in the specimen. They also found that the AE technique is a useful tool for AWJ material removal process monitoring and control of metals. Momber et al. (Ref 6) investigated the behavior of concrete exposed to hydroabrasive erosion using the AE technique. They showed that AE is a suitable method for online analysis of the erosion resistance of this type of material. They also found that AE signal parameters could be linked to mechanical properties of brittle precracked materials if they undergo an identical erosion mechanism. However, the investigation was performed on the macroscopic level, and the AE signals have not been linked to the microscopic material removal range.

The objective of this article is to demonstrate the capability of AE for online sensing material removal processes occurring on the microscopic level. If this capability is established, a major step will have been made toward the online monitoring of efficiency and quality of the AWJ machining of refractory ceramics and other difficult-to-machine materials.

2. Properties and Structure of the Investigated Material

Commercial bauxite refractory ceramic bricks, commonly used as lining materials in the steel industry, were investigated in this study. Table 1 lists the mechanical properties of the material. Table 2 gives the chemical compositions. From the point of view of phase composition, the material mainly contains corundum (50 to 70%) and mullite (25 to 35%). It has a medium Young's modulus and a relatively high compressive strength. Generally the temperature resistance is low.

Table 1 Mechanical properties of the test material

Properties	Value
Young's modulus, MPa	59,000
Cold compressive strength, MPa	126
Cold bending strength, MPa	19
Density, kg/m^3	2,890
Porosity, %	17

A.W. Momber, WOMA Apparatebau GmbH, Duisburg, Germany; **R.S. Mohan,** The University of Tulsa, Department of Mechanical Engineering, Tulsa, OK; and **R. Kovacevic,** Southern Methodist University, Department of Mechanical Engineering, Dallas, TX. Contact e-mail: AMomber@iris.swin.eu.au.

Prior to the cutting experiments, the structure of several samples was examined by x-ray spectroscopy and SEM. The chemical analysis identified the major mineral phases as α-corundum, mullite, tialite, and titanium oxide. The SEM image in Fig. 1 shows two large corundum grains (5 mm in length) that are sharply separated from the matrix by interfaces (grain boundaries are arrowed).

The matrix consists of corundum, mullite, and tialite. A close view on the matrix of the lower grain is given in Fig. 2, showing corundum grains (dark gray), and mullite (light gray). The very white reflecting areas are occupied by titanium oxide. The large corundum grains acting as inclusions consist of individual crystals, bonded by tialite and titanium oxide. The structure is porous.

3. Experimental Setup

The experimental setup consisted of an AWJ machining system, an AE sensor, a preamplifier, an A/D (analog to digital) converter, an AE monitoring system, and a PC/AT (personal computer/advanced technology) with suitable software. The AWJ system used for conducting the experiment consists of a high-pressure intensifier pump, an AWJ machining head, an abrasive metering and delivery system, an abrasive hopper with garnet as abrasive, a catcher tank, and an X-Y-Z positioning system controlled by a computer numerical control (CNC) controller. Figure 3 shows a schematic of the experimental setup. The AWJ parameters, namely pump pressure and traverse rate, were varied, and linear cuts were generated in the specimens.

Table 2 Chemical composition of the test material

Material	Percent
Al_2O_3	81.0
Fe_2O_3	1.7
SiO_2	12.0
$CaO + MgO$	0.4
TiO_2	3.2
$K_2O + Na_2O$	0.6

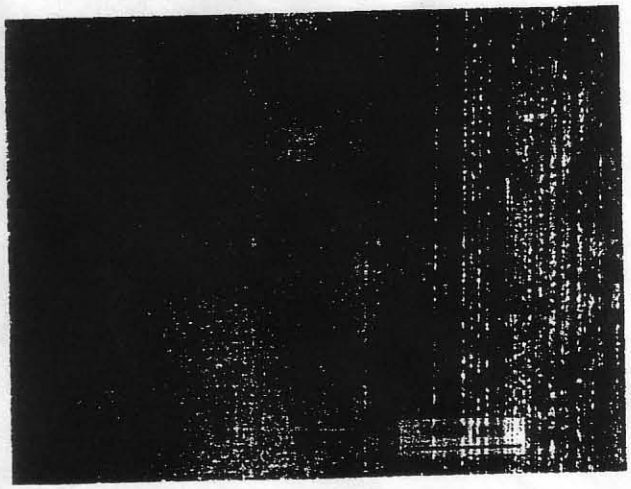

Fig. 1 Scanning electron microscopy image of the general bauxite structure. Note the sharply appearing interfaces. 20×

The generated AE signals were detected and processed by a model AET 5500 acoustic emission monitoring system (Babcock and Wilcox, sold by OnLine Digital Technologies, Inc., Carmicheael, CA), which consisted of an AET 5500 mainframe (signal processing unit), a graphics terminal (interface, data storage, and display), and the accessories (sensors, preamplifiers, etc.). When an acoustic emission caused by an induced stress occurred in a test specimen, the sensors (resonant frequency 2 MHz), fixed on top of the specimens, converted this acoustic emission wave into a voltage signal, which was amplified by the preamplifier and sent to the mainframe (16 bit microprocessor) for post processing. The distance between cut and sensor, which was fixed on the samples with a water resistant epoxy adhesive, was between 5 and 90 mm. The raw signal from the AE-monitoring system was acquired at a 1 MHz sampling frequency (with a gain of 1.0 and 5.0, respectively) using a suitable personal computer based data acquisition system for spectrum analysis. Each data set consisted of 1024 discrete time domain points. Five data sets of the fast fourier transform

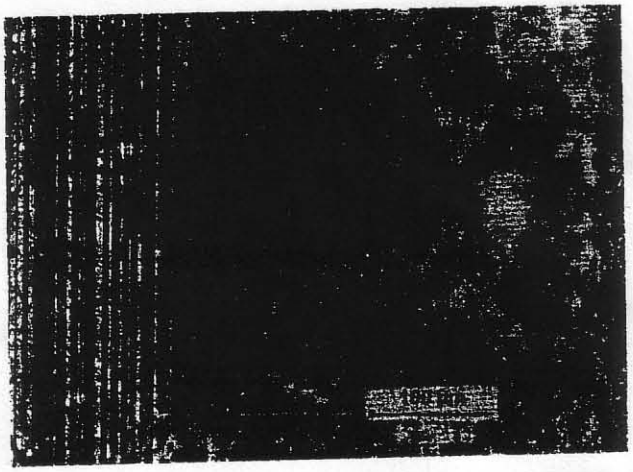

Fig. 2 Scanning electron microscopy image of the matrix material. 200×

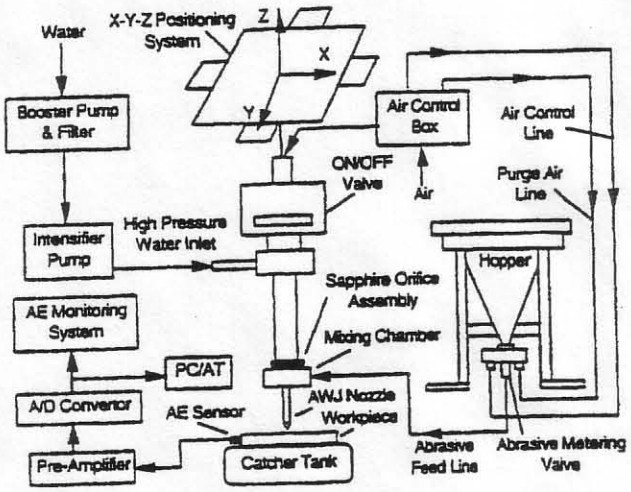

Fig. 3 Experimental setup

(FFT) of the time domain signals acquired under the same experimental conditions were averaged, and the representative signal was obtained for analysis.

After cutting, parts of the specimens were embedded in resin and examined by optical microscopes with magnifications between 35 and 140× as well as by SEM.

4. Experimental Results and Discussion

4.1 Material Removal Process Observations

Figure 4 illustrates the structure after AWJ cutting at 100 MPa. Two inclusion grains can be distinguished in the middle of the figure (marked by arrows), containing several mineral phases (mullite, tialite) illustrated by the accumulation of dark spots. These grains have been cut by the AWJ. In contrast, the grain on the extreme right, consisting of almost pure corundum, is undamaged. Here, only the matrix material has been removed. Similar phenomena can be noticed in the left section, where the large corundum inclusion is partly exposed but not cut.

Figure 5 provides further evidence. Here, an exposed corundum grain is shown as well as evidence that the surrounding matrix material is removed by the abrasive water jet. The corundum grain is still rounded, which suggests that it was probably pulled out by the action of the flowing water in the kerf after the matrix was removed.

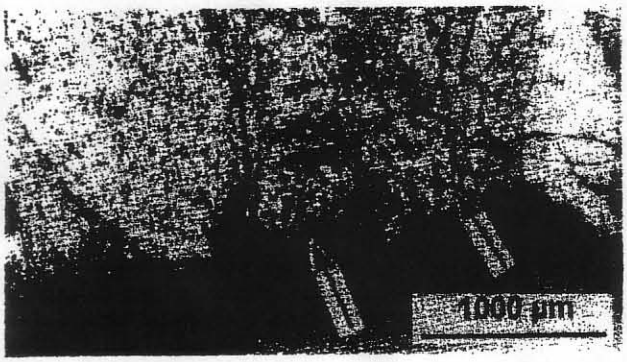

Fig. 4 Optical microscope image of the bauxite structure cut by abrasive water jet (AWJ). 35×

Fig. 6 Scanning electron microscopy image of a corundum grain broken by abrasive water jet (AWJ). 500×

Figure 6 presents a close view of a corundum grain cut by AWJ machining. A striking feature is that the corundum crystals are unbroken. Obviously they are separated from the surrounding tialite matrix by intergranular fracture in the interface region.

Table 3 Abrasive water jet cutting conditions

Conditions	Values
Fixed parameters	
Abrasive material	Garnet
Abrasive size	No. 36
Abrasive particle shape	Angular
Orifice material	Sapphire
Orifice diameter, mm	0.457
Focus length, mm	89.0
Focus diameter, mm	1.27
Stand-off distance, mm	6.0
Method of feed	Suction
Abrasive condition	Dry
Abrasive flow rate, g/s	7.41
Jet impact angle	90°
Variable parameters	
Pump pressure, MPa	100, 150, 200
Traverse rate, mm/s	0.5, 1.0

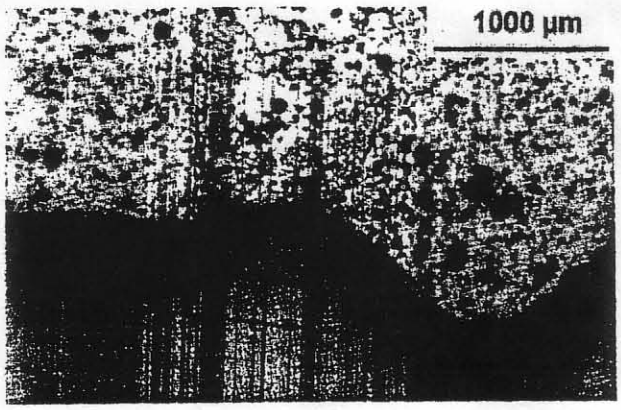

Fig. 5 Optical microscope image of corundum grains attacked by abrasive water jet (AWJ). 35×

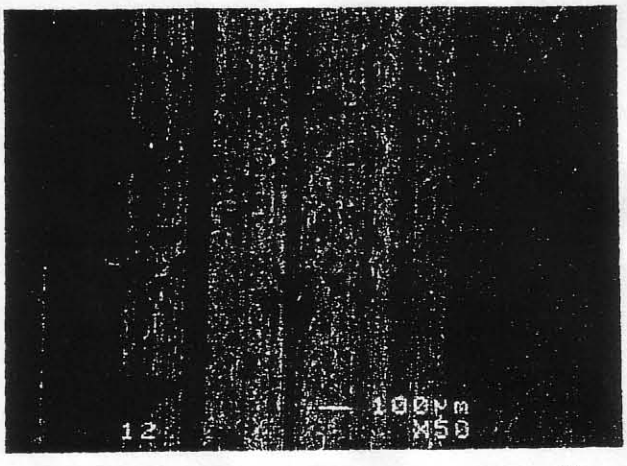

Fig. 7 Scanning electron microscopy image of transcrystalline cut bauxite (scale: 100 µm)

The situation is different for the material cut at a higher pump pressure level. Figure 7, which is a SEM image from the upper part of the cut, shows, for example, that the grain boundary at the corundum grains remains intact after the abrasive water jet attack. The failure runs completely through both the grains and the matrix.

Two major conclusions can be drawn from this investigation. First, the machining of bauxite by AWJ is an unsteady material removal process, covering matrix removal, interfacial failure, and inclusion fracture by crystal separation. Second, if a certain pump pressure (or a certain local stress value) is exceeded, inclusion failure by crystal fracture in single-phase corundum inclusion attributes to the material removal. As the acoustic emission signal is capable of identifying microscopic changes in the energy dissipation process (Ref 5), both features should be detectable by online AE measurements during the cutting process.

4.2 *Acoustic Emission Measurements during Cutting*

The unsteady material removal process is reflected by the structure of the time domain acoustic emission signals acquired during cutting at different pressures. As shown in Fig. 8 and 9, the acoustic emission signals exhibit several burst emissions. This type of emission usually corresponds to events of sudden energy release, such as spalling fracture. Probably the burst emissions are expressions of inclusion grain fracture. This process can generate high energy stress waves, which are detected by the acoustic emission technique.

Nevertheless, in Fig. 8(a), for a pump pressure of 100 MPa, just two major burst emissions can be noticed, with a maximum amplitude of ±8 V and a duration of approximately 0.05 ms. The corresponding frequency domain signal is widely spread but shows a peak at approximately 130 kHz (Fig. 8b). A different situation can be found as the pump level is doubled. Figure 9(a), containing time domain signals acquired at a pressure of p = 200 MPa, shows an increased amount of burst emissions, approximately seven. The maximum amplitude of the emissions is ±12 V, and the average duration increases up to 0.08 ms. Even more pronounced are the modifications in the frequency domain signal (Fig. 9b). Here a second peak, located at a frequency of approximately 250 kHz, can clearly be distinguished.

The same effect was observed as the traverse rate was decreased during cutting. Figure 10 illustrates this, showing the frequency domain signals. For the high traverse rate, signals

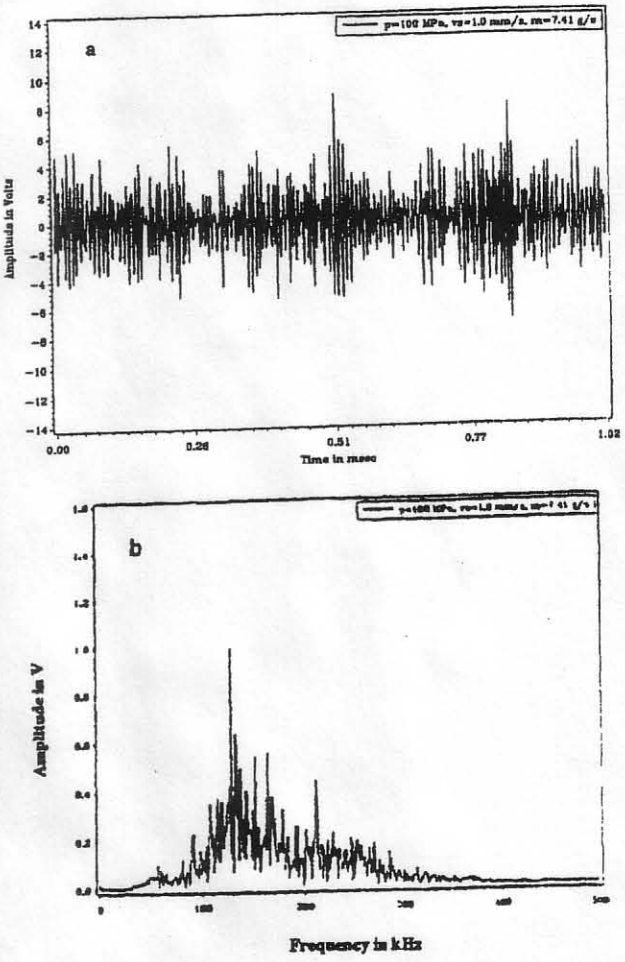

Fig. 8 Acoustic emission signals, acquired at p = 100 MPa (gain: 5). (a) Time domain. (b) Frequency domain

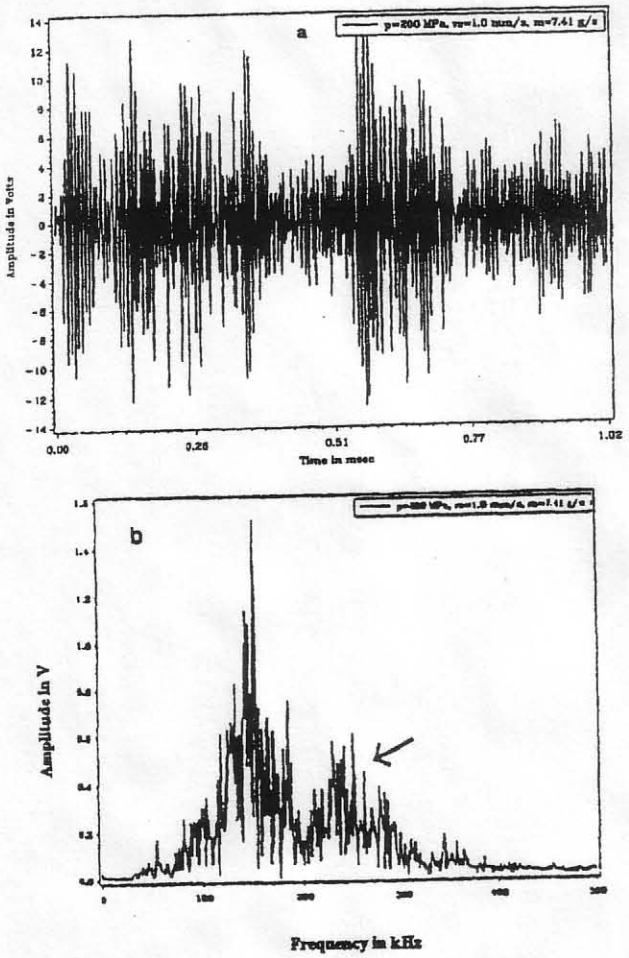

Fig. 9 Acoustic emission signals, acquired at p = 200 MPa (gain: 5). (a) Time domain. (b) Frequency domain

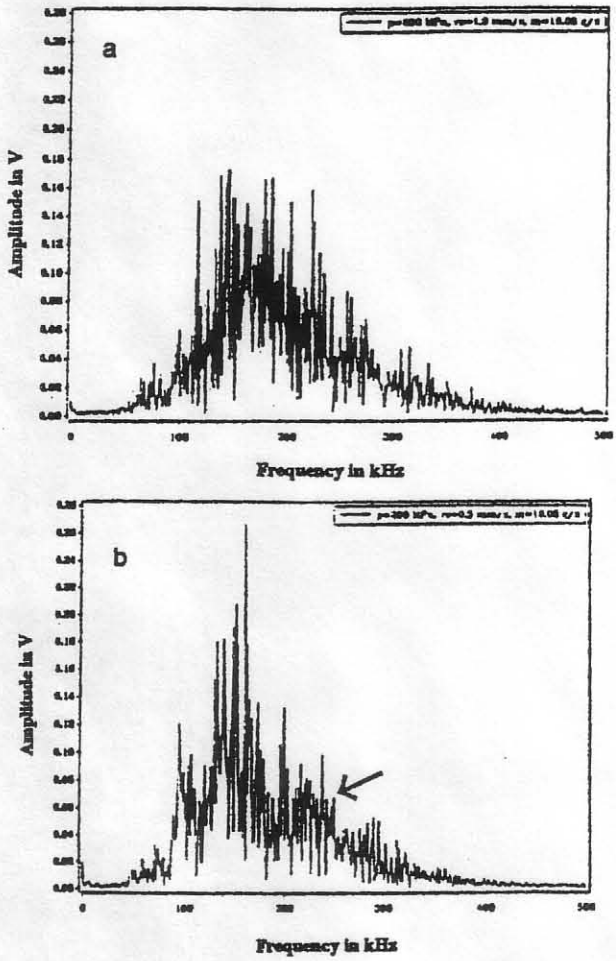

Fig. 10 Frequency domain AE signals, acquired at different traverse rates (gain: 1). (a) 1.0 mm/s. (b) 0.5 mm/s

are grouped around a frequency of 150 kHz (Fig. 10a). As the traverse rate decreases, the second peak at a frequency of 250 kHz appears again (Fig. 10b).

Pump pressure, p, and traverse rate, v, are correlated with the abrasive water jet kinetic energy, E_A, by Ref 1:

$$E_A \propto p^{1.5} \cdot v^{-1} \quad \text{(Eq 1)}$$

Thus, an increase in pressure and a decrease in traverse rate caused the kinetic energy to increase. The two-peak characteristics of the AE signals are therefore typical for high energy levels. The AE signals support the conclusions drawn from the microphotographs very well. First, an unsteady material removal process is confirmed. The burst emission in the signals could be due to the intercrystalline fracture of the multiphase corundum grains; whereas, the basic signal can be linked to matrix removal as well as to the interfacial pullout of the plain corundum grains. As the jet energy increased, the plain corundum inclusions were also broken. Additionally, transcrystalline fracture may occur in the multiphase corundum. Both events add an additional failure mode to the removal process, which is expressed by the increased number of burst emissions in the time domain signal as well as in the second peak in the frequency domain signal. Interestingly, the second peak appears at higher frequencies. A probable reason could be the much smaller dimensions, and thus the larger number of the corundum crystals compared to the inclusion grains.

5. Conclusions

The results of the study can be summarized as follows:

- Abrasive water jets can generally be used to efficiently machine bauxite refractory ceramics.
- The material removal process is a mixture between transgranular fracture and interfacial grain pullout. The amount of both modes on the general material removal process depends on the energy delivered by the abrasive water jet.
- The preliminary attempt to control the material failure process on the microscopic level by the AE technique delivers most promising results. Acoustic emission signals are very sensitive to changes in material removal modes.

Acknowledgments

The authors are grateful to the Alexander-von-Humboldt Foundation, Bonn, Germany, and to the Center for Robotic and Manufacturing Systems, University of Kentucky, Lexington, KY, for financial support. Thanks are given to I. Eusch for his help in the experimentation. The authors also appreciate the use of facilities at Montan Universität Leoben, Institut für Gesteinshüttenkunde, Austria, where scanning electron microscopy and x-ray spectroscopy were completed.

References

1. A.W. Momber and R. Kovacevic, *Principles of Abrasive Water Jet Machining*, Springer-Verlag, 1998
2. A.W. Momber, I. Eusch, and R. Kovacevic, *J. Mat. Sci.*, Vol 31, 1996, p 6485
3. R. Kovacevic, H. Kwak, and R.S. Mohan, *IME J. Eng. Manuf.*, Vol 212, 1998, p 45
4. R.S. Mohan, A.W. Momber, and R. Kovacevic, *Jet Cutting Technology*, N.S. Allan, Ed., Mechanical Engineering Publications, 1994, p 649
5. R.S. Mohan, A.W. Momber, and R. Kovacevic, *IME J. Eng. Manuf.*, in review, 1999
6. A.W. Momber, R.S. Mohan, and R. Kovacevic, *Theoret. Appl. Fracture Mech.*, Vol 31, 1999, p 1